ISSN: 2395-7852

International Journal of Advanced Research in Arts, Science, Engineering & Management

Volume 13, Issue 1, January – February 2026

INTERNATIONAL STANDARD SERIAL NUMBER INDIA

Impact Factor: 8.028

+91 9940572462 +91 9940572462 ijarasem@gmail.com www.ijarasem.com

International Journal of Advanced Research in Arts, Science, Engineering & Management (IJARASEM)

| ISSN: 2395-7852 | www.ijarasem.com | Impact Factor: 8.028 | Bimonthly, Peer Reviewed & Refereed Journal|

| Volume 13, Issue 1, January – February 2026 |

Design and Fabrication of Perovskite-Sensitized Solar Cells: Assessing Photovoltaic Performance

Surendra Kumar Saini[1], Dr. Anshul Joon[2], Dr. Mohit Kumar[3]

Research Scholar, Department of Physics, SKD University, Hanumangarh, India[1]

Supervisor, Department of Physics, SKD University, Hanumangarh, India[2]

Co-Supervisor, Department of Physics (Guest faculty), Govt Girls College, Hanumangarh , India[3]

ABSTRACT: The present study reports the design, fabrication, and photovoltaic performance assessment of perovskite-sensitized solar cells (PSCs/PSSCs) using lead-free tin-based perovskite materials. $MASnI_3$ and $MASnCl_3$ were synthesized and employed as photosensitizers in DSSC-type device architectures. The study demonstrates the promising potential of lead-free tin-based perovskite sensitizers for photovoltaic applications and underscores the importance of halide composition in optimizing device performance.

KEYWORDS: Perovskite-sensitized solar cells; Methylammonium tin iodide ($MASnI_3$); Methylammonium tin chloride ($MASnCl_3$); Photovoltaic performance.

I. INTRODUCTION

The rapid depletion of fossil fuel resources and the growing concerns over climate change have intensified global efforts to develop clean, sustainable, and renewable energy technologies. The literature underscores the challenges that must be surmounted to attain a more sustainable and equitable future, including the enhancement of energy accessibility and the mitigation of carbon emissions (Prajapati et al., 2025; Pithale, 2025; Chaturvedi et al., 2024; Srivastava and Reddy, 2022; Singh and McGregor, 2025). Thus, solar energy has emerged as one of the most promising alternatives due to its abundance, environmental friendliness, and long-term sustainability. Over the past few decades, extensive research has been carried out to improve the efficiency, stability, and cost-effectiveness of solar cells, leading to the development of several generations of photovoltaic devices. Photovoltaic technologies offer a direct means of converting solar radiation into usable electrical energy; however, conventional silicon-based solar cells face limitations related to high production costs, energy-intensive manufacturing processes, and material constraints. As a result, next-generation photovoltaic technologies such as PSCs have emerged as promising alternatives due to their lower cost, simpler fabrication, and potential for high efficiency. In view of this, the present study aims to synthesize perovskite materials for solar cell application.

II. MATERIAL AND METHODS

Chemicals and Equipment:

The present study employed chemicals of analytical grade (AR grade), while some reagents of laboratory grade (LR grade) were used based on their ready availability in the laboratory. The chemicals utilized in the investigation are listed in the table 1.

Table 1: List of Chemicals

S. No.	Chemical / Material	Details
1	Titanium Dioxide (Anatase)	Purity: 99.9%
2	Fluorine-doped Tin Oxide Glass	Dimension: 50 mm × 50 mm × 2.2 mm. Resistivity: 7 Ohms/sq.
3	Ethanol	-
4	Distilled / Deionized Water	-
5	Methylamine Solution	-
6	Hydroiodic Acid	-

7	Methylammonium Iodide	-
8	Methylammonium Chloride	-
9	Tin Powder	-
10	Iodine	-
11	Tin (II) Iodide	-
12	Tin (II) Chloride	-
13	Diethyl Ether	-
14	Acetone	-
15	2-Propanol (Isopropyl Alcohol)	-
16	RBS 25 Solution	-
17	Potassium Iodide	-
18	Graphite (Pencil Lead)	-
19	Polyaniline	-
20	Thiourea	-
21	Ethylene Glycol	-

Table 2 provides the list of equipment and instruments used in the study.

Table 2: List of Equipment and Instruments

S. No.	Equipment and Instruments
1	Ammeter
2	Analytical balance
3	Digital Multimeter
4	Electric furnance
5	Glassware-Borosil
6	Hot Plate
7	Magnetic stirrer
8	Potentiometer (470K)
9	Shimadzu IR AFFINITY-1
10	Voltmeter

Fabrication of DSSC:

In the present study, the fabrication of DSSC is done using the steps given in figure 1.

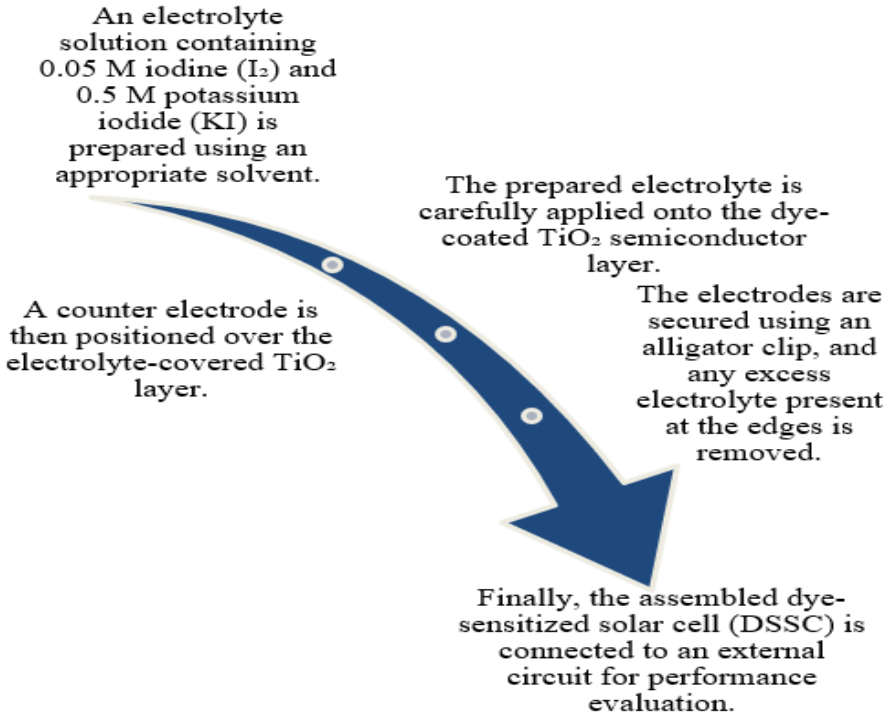

Fig 1: Assembly of DSSC

Electrolyte: In the present study, a potassium iodide–iodine (KI + I_2) solution was employed as the electrolyte, which was prepared following the procedure illustrated in the figure 2.

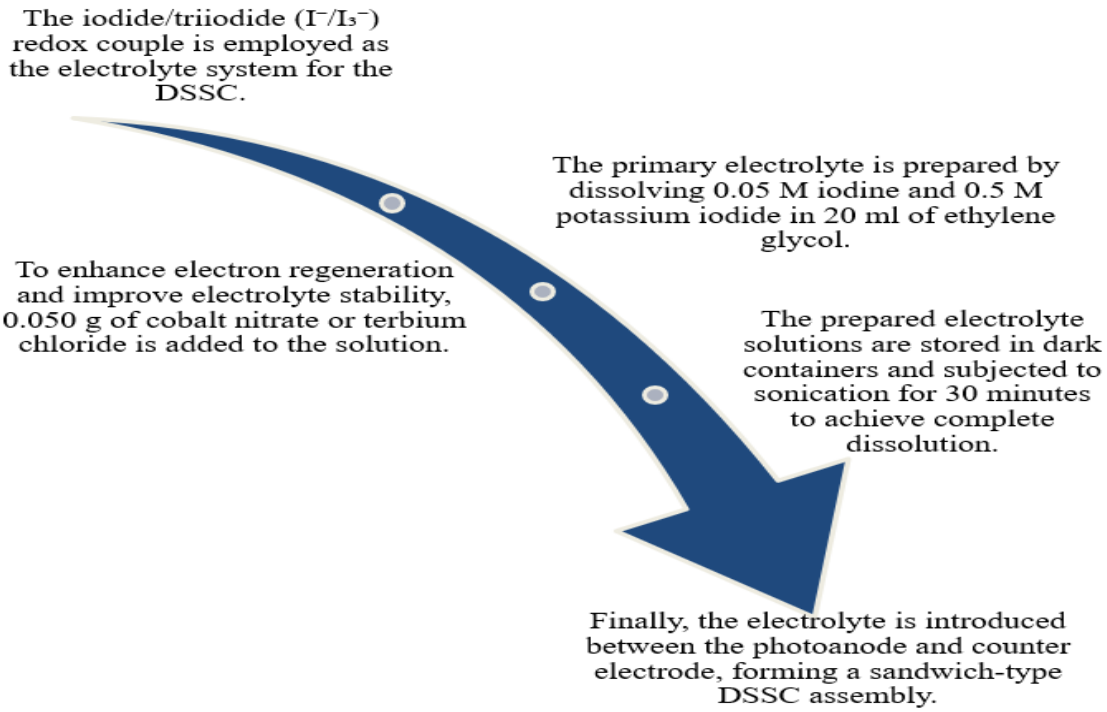

Fig 2: Preparation of Electrolyte

Photosensitizers: The following materials were used as Photosensitizers in the solar cell fabrication.

$MASnI_3$ - Methylammonium tin iodide ($CH_3NH_3SnI_3$) was prepared via a stepwise process involving the independent synthesis of methylammonium iodide (MAI) and tin(II) iodide (SnI_2), followed by the formation of perovskite films on conductive substrates. Initially, methylammonium iodide was synthesized by reacting a methylamine solution (33 wt.% in ethanol) with hydroiodic acid (57 wt.% in water) in a round-bottom flask maintained at 0 °C. The reaction was allowed to proceed for 2 h, after which the solvents were removed by distillation at 50 °C. The resulting crude product was dissolved again in ethanol and precipitated using diethyl ether, followed by filtration. This purification step was repeated several times to obtain a high-purity product. The purified CH_3NH_3I was then sublimed at 120 °C and stored under a dry nitrogen atmosphere in a glovebox to protect it from moisture.

Tin(II) iodide was synthesized separately by refluxing tin powder with iodine in 2 M hydrochloric acid at 115 °C in a round-bottom flask. The gradual change of the solution to a yellow color indicated the formation of SnI_2. The hot reaction mixture was filtered through glass wool into a preheated flask and allowed to cool slowly to ambient temperature, during which orange–red SnI_2 crystals crystallized out. These crystals were collected by filtration, washed with a water–hydrochloric acid mixture, dried under vacuum at 150 °C, and preserved under dry nitrogen to prevent oxidation.

For the fabrication of perovskite films, fluorine-doped tin oxide (FTO)-coated glass substrates were thoroughly cleaned using RBS 25 solution, acetone, and 2-propanol in an ultrasonic bath and subsequently stored in 2-propanol. A thin layer of tin(II) iodide, approximately 100 nm in thickness, was deposited onto the cleaned FTO substrates by thermal evaporation at a controlled rate under high vacuum. The SnI_2-coated substrates were immediately transferred into a nitrogen-filled glovebox without any exposure to air. A solution of methylammonium iodide in 2-propanol was then spin-coated onto the SnI_2 layer. During spin coating, MAI reacted rapidly with SnI_2, leading to the formation of dark brown to nearly black $CH_3NH_3SnI_3$ perovskite films. In certain cases, the films were annealed at temperatures between 60 and 100 °C to enhance film quality, although annealing was not strictly required for perovskite formation. FTO-coated glass was used as a standard conductive substrate due to its surface roughness, which closely resembles that of practical solar cell devices. Furthermore, SnI_2 was also deposited on compact and mesoporous TiO_2 substrates, producing perovskite films with similar morphology, albeit with slightly increased light-scattering characteristics.

$MASnCl_3$ - Methylammonium chloride (CH_3NH_3Cl) was prepared by reacting 30 mL of methylamine solution (40% in methanol) with 32.3 mL of hydrochloric acid (57 wt.% in water) in a 250 mL round-bottom flask maintained at 0 °C under continuous stirring for 2 hours. After completion of the reaction, the resulting precipitate was collected by evaporating the solvents using a rotary evaporator at 50 °C. The crude yellowish CH_3NH_3Cl product was purified by washing with diethyl ether while stirring for 30 minutes. This washing process was repeated three times, followed by recrystallization using a mixed solvent system of diethyl ether and ethanol. Subsequently, 0.395 g of the purified CH_3NH_3Cl was combined with 1.157 g of tin(II) chloride ($SnCl_2$) and stirred continuously at 60 °C overnight. After mixing, the reaction vessel was tightly sealed and kept in the dark at room temperature by wrapping it with aluminum foil to prevent any undesired photochemical reactions.

Fabrication of working electrode/ Photoanode: In the present study, a TiO_2 paste was used for photoanode fabrication, and its preparation procedure is illustrated in the accompanying figure 3.

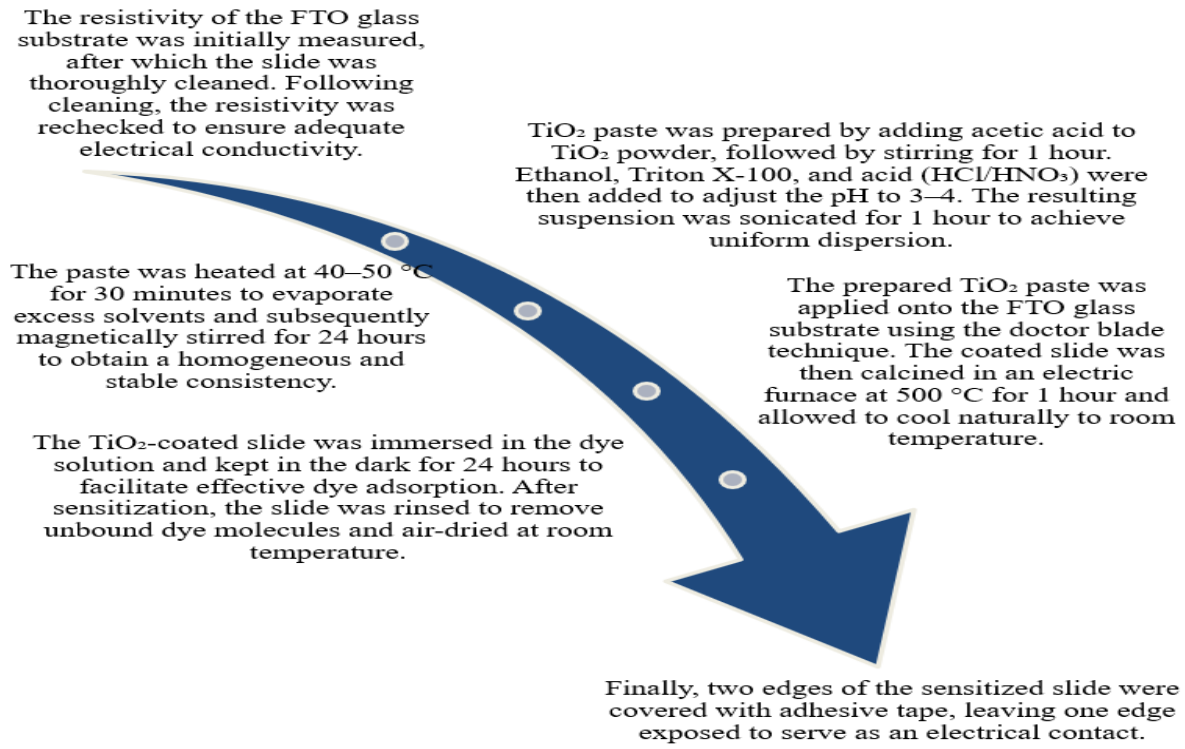

Fig 3: Preparation of Photoanode using TiO_2

Counter Electrode (Graphite): Owing to the high cost of platinum, this study employed graphite as a cost-effective alternative for the counter electrode. The graphite counter electrode was placed adjacent to the photoanode and held in position using clips, and it was fabricated using pencil graphite as the electrode material.

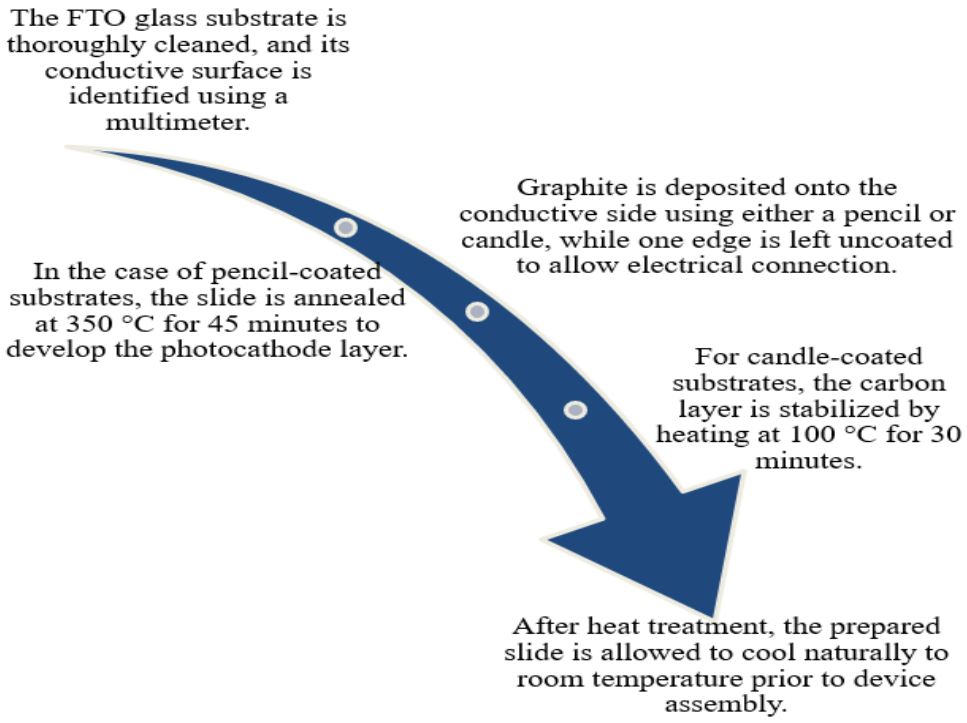

Fig 4: Preparation of Graphite counter electrode

IR Characterization:
In the present study, FTIR analysis was carried out using a Shimadzu IR AFFINITY-1 spectrophotometer operating in the range of 4000–600 cm^{-1}.

J-V Characterization:
The prepared DSSCs were tested under artificial illumination provided by a halogen lamp, and their electrical performance was systematically assessed. Important photovoltaic parameters, namely open-circuit voltage (Voc), short-circuit current density (Jsc), maximum power output (Pmax), fill factor (FF), and overall power conversion efficiency, were obtained from the I–V measurements. The adopted approach highlights the use of mixed dye systems in combination with surfactants and metal salts to enhance light absorption over a wider spectral range, improve charge transfer processes, and optimize overall device performance. Moreover, the use of low-cost materials and simple fabrication procedures provides a practical and scalable pathway for the advancement of DSSC technology. The following parameters were evaluated to calculate the efficiency of the synthesized DSSCs.

1. **V_{oc} (open-circuit voltage):** Voc represents the maximum voltage produced by a solar cell when there is no external current flow. It corresponds to the voltage at which the net current in the I–V curve becomes zero.
2. **J_{sc} (current density):** Jsc is defined as the the maximum photocurrent per unit area generated under short-circuit conditions (zero voltage).
3. **$P_{max.}$ (maximum power point):** The maximum power output occurs at a specific operating point characterized by voltage (Vpp) and current (Ipp), and is expressed as:

$$P_{max.}) = V_{pp} * I_{pp}$$

4. **FF (fill factor):** The fill factor provides a measure of the quality and stability of the solar cell, with higher FF values indicating better performance. The fill factor is given by:

$$FF = V_{pp} * I_{pp} / J_{sc} * V_{oc}$$

5. **Efficiency of the Cell (η):** The power conversion efficiency (η) is a crucial parameter that represents the ability of the DSSC to convert incident light energy into electrical energy and is calculated using the standard efficiency expression:

$$\eta = \frac{FF \times J_{sc} \times V_{oc}}{P_{in}} \times 100$$

III. RESULT AND DISCUSSION

The FTIR spectrum of methylammonium tin iodide ($CH_3NH_3SnI_3$), shown in figure 5, confirms the successful formation of the organic–inorganic perovskite structure through the presence of characteristic vibrational bands associated with the methylammonium ($CH_3NH_3^+$) organic cation and its interaction with the inorganic tin halide framework. FTIR spectroscopy is particularly useful in identifying functional groups related to the organic component of perovskite materials, as the metal–halide lattice vibrations are generally IR inactive or appear at very low frequencies. A broad and intense absorption band observed in the region of 3500–3300 cm^{-1}, with a prominent peak around 3354 cm^{-1}, is attributed to the N–H stretching vibrations of the ammonium (NH_3^+) group present in the methylammonium cation. This strong N–H stretching band indicates the successful incorporation of the organic cation into the perovskite lattice and reflects hydrogen bonding interactions between the NH_3^+ group and the surrounding halide ions. Such hydrogen bonding plays an important role in stabilizing the perovskite structure.

The absorption band observed near 2919 cm^{-1} corresponds to the C–H stretching vibrations of the methyl (CH_3^+) group. This confirms the presence of the alkyl component of the methylammonium cation within the $MASnI_3$ structure. Additionally, a band around 1620 cm^{-1} is assigned to the symmetric and asymmetric bending vibrations of N–H, further supporting the existence of the protonated ammonium group. The peaks appearing near 1548 cm^{-1} are associated with the symmetric and asymmetric bending modes of C–H bonds, which are characteristic of organic ammonium salts. Furthermore, the presence of a band around 1246 cm^{-1} corresponds to C–N stretching vibrations, providing additional confirmation of the methylammonium framework within the perovskite material. Although halide-related vibrations are generally weak in FTIR spectra, low-frequency bands observed in the region below 700 cm^{-1} can be attributed to organic–halide interactions and lattice-associated vibrations, indirectly confirming the formation of the tin halide perovskite network. In previously reported studies, similar low-wavenumber features have been linked to alkyl halide–related stretching modes, supporting the integrity of the perovskite structure.

| ISSN: 2395-7852 | www.ijarasem.com | Impact Factor: 8.028 | Bimonthly, Peer Reviewed & Refereed Journal|

| Volume 13, Issue 1, January – February 2026 |

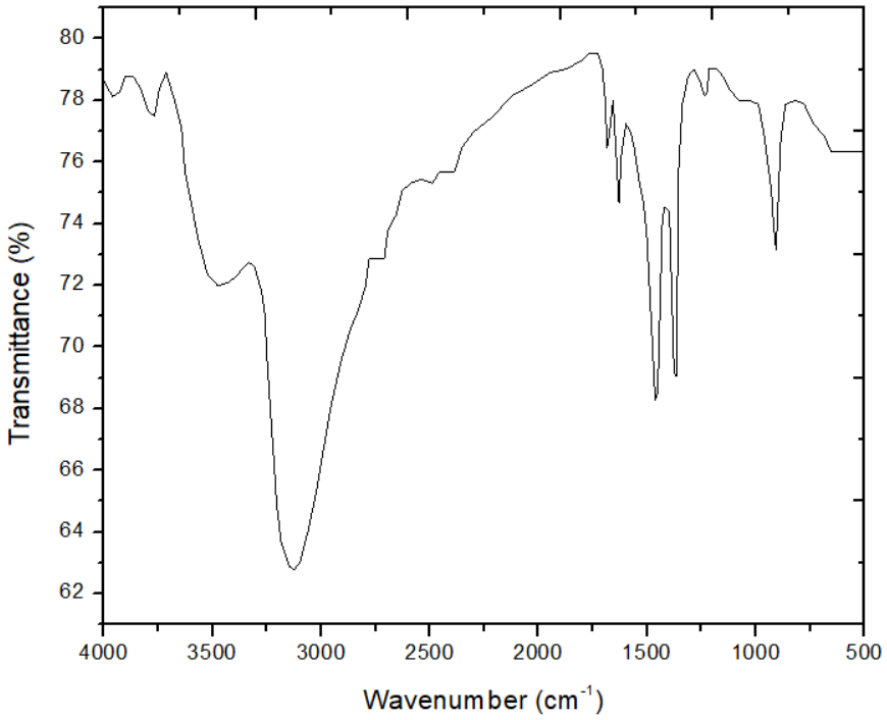

Fig 5: FTIR spectrum of $MASnI_3$ dye

The FTIR spectrum of methylammonium tin chloride ($CH_3NH_3SnCl_3$), shown in figure 6, provides clear evidence for the successful formation of the organic–inorganic perovskite structure through the identification of characteristic vibrational modes associated with the methylammonium ($CH_3NH_3^+$) cation. As in other hybrid perovskites, the FTIR response is dominated by vibrations of the organic component, while the inorganic Sn–Cl framework contributes mainly to low-frequency lattice vibrations. A broad and intense absorption band observed in the 3500–3300 cm^{-1} region is attributed to the N–H stretching vibrations of the NH_3^+ group of the methylammonium cation. This broad feature indicates strong hydrogen bonding interactions between the ammonium protons and chloride ions in the perovskite lattice, which play a crucial role in stabilizing the crystal structure. The presence of this band confirms the successful incorporation of the organic cation into the $SnCl_3^-$ framework.

Distinct absorption peaks appearing around 2920–3000 cm^{-1} correspond to the C–H stretching vibrations of the methyl (CH_3^+) group. These vibrations are characteristic of alkyl ammonium salts and confirm the presence of the methyl group in the perovskite structure. Additionally, the band observed near 1620–1650 cm^{-1} is assigned to the symmetric and asymmetric bending modes of the N–H bonds, further supporting the existence of the protonated ammonium group. The absorption features around 1540–1550 cm^{-1} are associated with C–H bending vibrations, while bands appearing in the region of 1250–1300 cm^{-1} correspond to C–N stretching vibrations of the methylammonium cation. These peaks collectively confirm the integrity of the organic moiety within the $MASnCl_3$ structure. Notably, strong absorption bands observed in the 600–700 cm^{-1} region are attributed to C–Cl stretching vibrations, which are characteristic of alkyl halide interactions. These bands indicate the presence of chloride ions interacting with the organic cation and indirectly confirm the formation of the tin chloride perovskite lattice. Such low-wavenumber features are commonly reported for chloride-based perovskites and differentiate $MASnCl_3$ from its iodide counterpart.

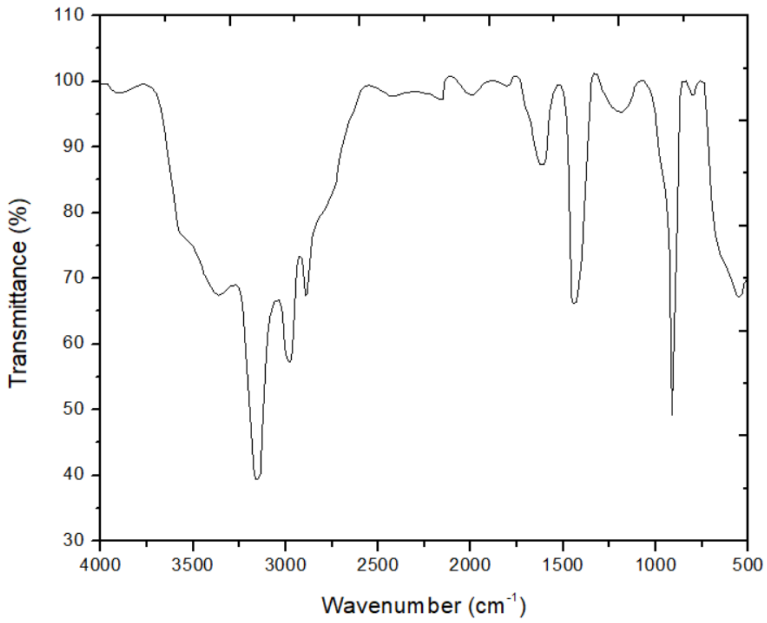

Fig 6: FTIR spectrum of $MASnCl_3$ dye

The perovskite-based sensitizers exhibited significant photovoltaic performance. Among them, $MASnI_3$ delivered the best overall performance, with a Voc of 0.933 V, Jsc of 20.058 mA, FF of 0.483, and a η of 9.046%. The superior efficiency of $MASnI_3$ can be attributed to its narrow bandgap, strong and broad absorption across the visible spectrum, high charge-carrier mobility, and efficient electron injection into the TiO_2 conduction band. The relatively high current density indicates excellent light-harvesting capability and efficient charge generation. $MASnCl_3$ exhibited inferior performance to $MASnI_3$. The device sensitized with $MASnCl_3$ showed a Voc of 0.842 V and an Jsc of 11.241 mA; however, the fill factor was comparatively low (0.352), resulting in a moderate efficiency of 3.329%. The lower efficiency of $MASnCl_3$ can be attributed to its wider bandgap compared to $MASnI_3$, which limits light absorption, as well as higher recombination losses and reduced charge transport efficiency, reflected in the lower FF.

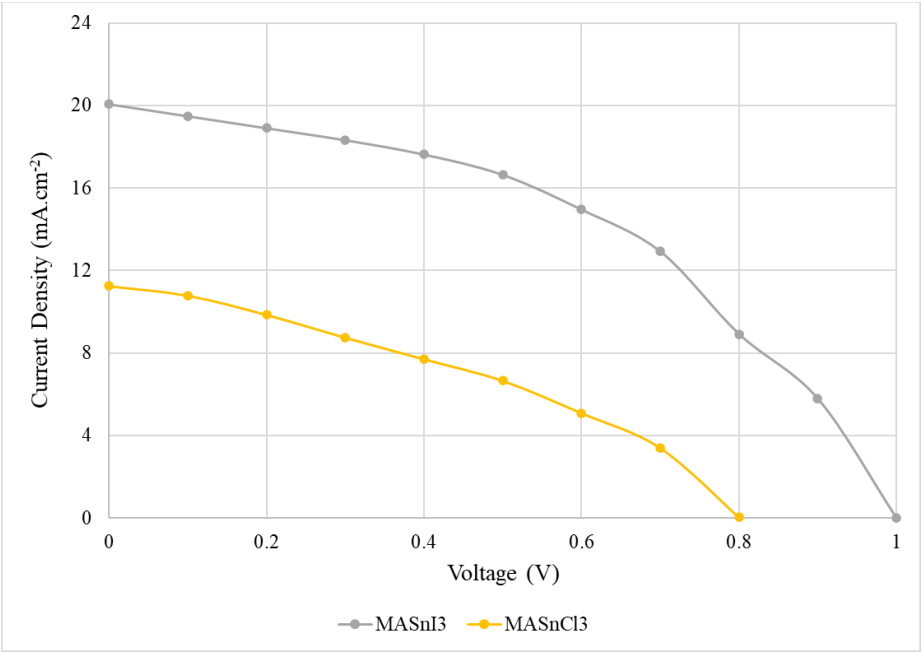

Fig 7: J–V Characteristics of DSSCs using perovskite sensitizers

Table 3: Photovoltaic parameters of DSSCs sensitized with perovskite materials

S. No.	Sample	V_{oc} (V)	J_{sc} (mA)	FF	η (%)
1	$MASnI_3$	0.933	20.058	0.483	9.046
2	$MASnCl_3$	0.842	11.241	0.352	3.329

The findings of the present study on tin-based perovskite sensitizers ($MASnI_3$ and $MASnCl_3$) are largely consistent with, and supportive of, earlier experimental and simulation-based investigations, while also highlighting certain practical limitations inherent to simple DSSC-type architectures. In the present work, FTIR analysis confirmed the successful formation of hybrid organic–inorganic perovskite structures for both $MASnI_3$ and $MASnCl_3$. The strong absorption bands observed in the 3500–3300 cm^{-1} region, attributed to N–H stretching vibrations of the methylammonium ($CH_3NH_3^+$) cation, are in excellent agreement with earlier reports on tin-based perovskites. Weiss et al. (2015) similarly emphasized the role of organic–inorganic interactions and hydrogen bonding in stabilizing $CH_3NH_3SnI_3$ films, noting that these interactions contribute to structural integrity and long-term material stability.

The presence of C–H stretching, N–H bending, and C–N stretching bands in the present FTIR spectra further corroborates the intact incorporation of the methylammonium cation within the perovskite lattice, consistent with the synthesis and characterization reported by Rahul et al. (2018) for $CH_3NH_3SnCl_3$. Low-wavenumber features related to Sn–I and Sn–Cl interactions observed in this study also align with previous FTIR, XRD, and SEM-based confirmations of tin halide perovskite network formation. Thus, structurally and chemically, the FTIR findings of the present study are fully aligned with established literature, confirming the successful synthesis of lead-free tin-based perovskites suitable for photovoltaic applications.

$MASnI_3$ exhibited the best performance, with a Voc of 0.933 V, Jsc of 20.058 mA, and an efficiency of 9.046%. This result is comparable to experimental efficiencies reported for early-generation or simplified perovskite devices. For instance, Tombe et al. (2017) reported efficiencies around 9.2% for solution-processed $MAPbI_3$ devices, indicating that the efficiency achieved with $MASnI_3$ in the present study is competitive despite the use of a tin-based, lead-free material and a relatively simple device configuration. The superior performance of $MASnI_3$ observed in this study is also consistent with Weiss et al. (2015), who reported a narrow bandgap (~1.23 eV) and broad solar absorption for $CH_3NH_3SnI_3$, enabling high photocurrent generation. The high Jsc obtained in the present work supports this observation and confirms the excellent light-harvesting capability of iodide-based tin perovskites. However, the efficiencies reported in simulation-based studies are significantly higher. Singh et al. (2025), Sharma et al. (2023), and Khan et al. (2024) reported power conversion efficiencies exceeding 30% for $MASnI_3$-based devices using SCAPS-1D simulations. These discrepancies are expected, as simulated devices assume ideal conditions, including optimized absorber thickness, low defect density, perfect interfaces, and advanced charge transport layers. In contrast, the present study employs experimentally fabricated devices with practical limitations such as interfacial recombination, moderate fill factors, and non-optimized layer thicknesses, resulting in lower—but realistic—efficiency values.

The comparative performance trend observed in the present study—$MASnI_3$ outperforming $MASnCl_3$—is also well supported by earlier literature. $MASnCl_3$ showed a moderate efficiency of 3.329%, primarily due to its wider bandgap and reduced visible-light absorption. Rahul et al. (2018) reported that $CH_3NH_3SnCl_3$ exhibits good structural and optical properties but comparatively lower photovoltaic performance than iodide-based counterparts, a conclusion that closely matches the present findings. Similar trends have been observed in mixed-halide and lead-based systems as well. Tombe et al. (2017) demonstrated that halide composition strongly influences device efficiency, with iodide-rich perovskites generally exhibiting higher photocurrents and efficiencies than chloride- or bromide-rich compositions due to improved absorption and charge transport. Recent studies have explored hybrid strategies to improve stability and performance, such as incorporating natural dyes into perovskite systems (Chukwuemeka et al., 2024). While such approaches showed improved fill factors and stability, the overall efficiencies remained very low (<0.05%). Compared to these results, the efficiencies achieved in the present study using pure $MASnI_3$ and $MASnCl_3$ sensitizers are substantially higher, reinforcing the superior intrinsic photovoltaic potential of tin-based perovskites.

IV. CONCLUSION

In this study, PSCs were successfully designed, fabricated, and evaluated using lead-free tin-based perovskite materials, namely methylammonium tin iodide ($MASnI_3$) and methylammonium tin chloride ($MASnCl_3$), as photosensitizers. The devices were fabricated using a TiO_2 photoanode, a KI/I_2 electrolyte, and a graphite counter electrode, employing simple and cost-effective fabrication techniques. FTIR characterization confirmed the successful formation of hybrid organic–inorganic perovskite structures in both $MASnI_3$ and $MASnCl_3$, evidenced by characteristic vibrational modes associated with the methylammonium cation and its interaction with the tin halide framework. These results validate the chemical integrity and structural suitability of the synthesized perovskite materials for photovoltaic applications. Photovoltaic performance analysis revealed that $MASnI_3$-based solar cells exhibited superior performance, achieving a high open-circuit voltage (0.933 V), Jsc (20.058 mA), and efficiency (η) of 9.046%. The enhanced performance of $MASnI_3$ is attributed to its narrow bandgap, strong visible-light absorption, efficient charge-carrier generation, and effective electron injection into the TiO_2 conduction band. In contrast, $MASnCl_3$-based devices showed moderate performance with an efficiency of 3.329%, primarily due to their wider bandgap, reduced light absorption, and higher recombination losses. Overall, the findings demonstrate that iodide-based tin perovskites are more effective sensitizers than their chloride counterparts in DSSC-type architectures. The study highlights the significant potential of lead-free tin-based perovskite materials for photovoltaic applications and provides a foundation for further optimization through interface engineering, improved charge transport layers, and enhanced device architecture to achieve higher efficiency and long-term stability.

REFERENCES

1. Pithale, R. K. (2025). India's challenges and obstacles in achieving net zero carbon emissions by 2070: An economic perspective. *International Journal for Research Trends and Innovation, 10*(2), A599–A608.
2. Prajapati, P., Guo, R., Cai, A., & Prasad, R. (2025). Navigating the energy transition in India: Challenges and opportunities towards sustainable energy goal. *Water–Energy Nexus, 9*, 1–18. https://doi.org/10.1016/j.wen.2025.07.004
3. Singh, V. P., & McGregor, C. (2025). Driving sustainable energy futures: Lessons from India and South Africa energy transition strategies. *Energy Policy, 209*, 114957. https://doi.org/10.1016/j.enpol.2025.114957
4. Chaturvedi, V., Ghosh, A., Garg, A., Avashia, V., Vishwanathan, S. S., Gupta, D., Sinha, N. K., Bhushan, C., Banerjee, S., Datt, D., Bansal, J., Pathak, M., Dhar, S., Singh, A. K., Khan, N., Rashmi, R. R., Agrawal, S., Agarwal, D., Singh, A., … Prasad, S. (2024). India's pathway to net zero by 2070: Status, challenges, and way forward. *Environmental Research Letters, 19*(11), 112501. https://doi.org/10.1088/1748-9326/ad7749
5. Chukwuemeka, E. J., Osita, N. A., Odira, A. O., Uchechukwu, U. C., Mimi, J. D., & Ikhioya, I. L. (2024). Performance and stability evaluation of low-cost inorganic methyl ammonium lead iodide ($CH_3NH_3PbI_3$) perovskite solar cells enhanced with natural dyes from cashew and mango leaves. *Advanced Journal of Chemistry, Section A, 7*(1), 27–40. https://doi.org/10.48309/ajca.2024.406961.1384
6. Khan, N. N., Fareed, M., Mirza, S. H., & Zulfiqar, M. (2024). Lead-free perovskite solar cell based on methyl ammonium tin iodide: Possible power conversion efficiency enhancement by device simulation. *Heliyon, 10*(5), e27321. https://doi.org/10.1016/j.heliyon.2024.e27321
7. Sharma, D., Mehra, R., & Raj, B. (2023). Enhancement in efficiency of methyl ammonium tin iodide-based perovskite solar cell using SCAPS-1D. *NANO, 18*(14). https://doi.org/10.1142/S1793292023501096
8. Singh, M., Singh, D., Pal, P., Singh, S., Singh, D., & Giri, B. S. (2023). Synthesis and performance evaluation of *Beta vulgaris* based dye-sensitized organic solar cell. *Environmental Technology & Innovation, 31*, 103220. https://doi.org/10.1016/j.eti.2023.103220
9. Srivastava, B., & Reddy, P. (2022). Transformation of India towards net zero targets: Challenges and opportunities. *Nimit Mai Review, 5*, 1–8.
10. Rahul, N., Singh, P. K., Singh, R., Singh, V., Bhattacharya, B., & Khan, Z. H. (2017). New class of lead-free perovskite material for low-cost solar cell application. *Materials Research Bulletin, 97*, 572–577. https://doi.org/10.1016/j.materresbull.2017.09.054
11. Tombe, S., Adam, G., Heilbrunner, H., Apaydin, D. H., Ulbricht, C., Sariciftci, N. S., Arendse, C. J., Iwuoha, E., & Scharber, M. C. (2017). Optical and electronic properties of mixed halide (X = I, Cl, Br) methylammonium lead perovskite solar cells. *Journal of Materials Chemistry C, 5*(7), 1714–1723. https://doi.org/10.1039/C6TC04830G
12. Weiss, M., Horn, J., Richter, C., & Schlettwein, D. (2016). Preparation and characterization of methylammonium tin iodide layers as photovoltaic absorbers. *Physica Status Solidi (A), 213*(4), 975–981. https://doi.org/10.1002/pssa.201532594

International Journal of Advanced Research in Arts, Science, Engineering & Management (IJARASEM)

| Mobile No: +91-9940572462 | Whatsapp: +91-9940572462 | ijarasem@gmail.com |